Catalytic Activity and Control of the Nascent Morphology of Polyethylenes Obtained with First and Second Generation of Ziegler–Natta Catalysts

A. MUÑOZ-ESCALONA,* J. G. HERNANDEZ, and J. A. GALLARDO,
Laboratorio de Polímeros, Centro de Química, Instituto Venezolano de Investigaciones Científicas, Apartado 1827, Caracas 1010A, Venezuela

Synopsis

The morphologies of the as-produced polyethylenes obtained by slurry polymerization process of ethylene in *n*-heptane, using heterogeneous conventional and supported Ziegler–Natta catalysts, were investigated. The ability of four different catalytic systems in controlling the size and shape of the nascent polymer particles were tested. The catalytic systems employed were: the original Ziegler type catalyst produced by reduction of $TiCl_4$ with Et_2AlCl, the Natta type catalyst $TiCl_3$–AA, the reduced $TiCl_4$ with the metal carbonyls [$Mo(CO)_6$ and $Mn_2(CO)_{10}$], and the supported $TiCl_4$ on three commercial silicas having different surface areas: Davison 951, 952, and also the Dart 1000. It was found that the carriers affect the catalytic activity of the final catalyst and also its kinetic behavior. The supported Ziegler–Natta catalysts control more easily the nascent polymer particles (size, shape, and porosity) than the conventional ones. In addition, the morphology of the catalysts and the subsequent polymer particles are closely related to the parent morphology of the silicas used as carriers. Furthermore, the nascent morphology of the polyethylenes obtained with the conventional $TiCl_4$–Et_2AlCl catalytic system can be modified by using different |Al|/|Ti| ratios, resulting in more dense, spherical, and bigger polymer particles by increasing this ratio. On the other hand, detailed studies on the texture or arrangement of the polymer particles reveal the existence of mainly two fine morphologies (globular and wormlike), which are the result of the order of the primary or elementary catalyst particles (microspheres and platelets), the force linking them together, and the activity of the polymerization centers placed on their surface.

INTRODUCTION

In the recent years a great effort has been made to understand how the polyolefins grow on the surface of heterogeneous Ziegler–Natta catalysts.[1–8] Industrial and academic reasons can be given for that interest. On one side, the elucidation of the growth mechanism of single polymer chains on the active centers of the catalyst and the process by which they become assembled to form the different morphologies could give valuable information on the very complex coordinative polymerization mechanism. On the other hand, by controlling the average size and size distribution, shape, bulk density, and porosity of the polymer particles, these can be more easily worked up, the reactor productivity can be enhanced, and the elimination of the pelletizing process in the manufacture of the polyolefins can be expected. This process is one of the most energy consuming steps in a polymer plant.

It has been previously reported that, for the catalyst systems β-$TiCl_3$ obtained by reduction of $TiCl_4$ with Al alkyl and for the $TiCl_3$–AA–Et_2AlCl, the polymer particles retain the shape of the original catalyst particles.[2,7] This ability of the

Journal of Applied Polymer Science, Vol. 29, 1187–1202 (1984)
 CCC 0021-8995/84/041187-16$04.00

catalyst to impose its shape on the as-produced polymer has been named replication phenomenon.

The macroscopical catalyst particles consist of loosely bounded agglomeration of small subparticles with diameter in the microns. The monomer diffuses through the pores into the aggregate of subparticles. The polymerization takes place at the active centers located on their surface, crystallizing the produced polymer as soon as it becomes insoluble in the reaction medium, producing the encapsulation of the catalyst subparticles. The pores are, therefore, filled with polymer, leading to the fissuring, rupture, and expansion of the particles. The diameter of the polymer particles grows to a factor, several times the size of the catalyst particles, as the conversion increases (replication factor).[9]

In the case of the catalytic system based on $TiCl_4$–AA, we have shown[8,10] that the different nascent morphologies (globules and wormlike) are basically made up by the different aggregations of essentially two types, primary or elementary polymer subparticles (platelets and microspheres) produced by very tiny catalyst particles of the same shape, which remain embedded within them during the polymerization. Therefore, the variety of morphologies mentioned depends, consequently, on the manner by which these primary catalyst particles are arranged with respect to each other and also to their activity (polymerization rate). In the present paper we offer more evidence gathered not only with the $TiCl_3$ but also by using other catalytic systems, such as $TiCl_4$ reduced with Et_2AlCl and metal carbonyls [$Mo(CO)_6$ and $Mn_2(CO)_{10}$] and the supported $TiCl_4$ on three different commercial silicas: Davison 951, 952, and also the Dart 1000.

EXPERIMENTAL

Catalyst Preparations. Brown β-$TiCl_3$ was prepared by reduction of titanium tetrachloride (Merck, West Germany) with diethyl aluminum monochloride (Ethyl Co., United States) in the polymerization medium at 25°C, under stirring and using |Al|/|Ti| ratios within the range of 5–40. A suspension of porous catalyst particles in *n*-heptane was obtained, which could be easily stirred.

The reduction of $TiCl_4$ with $Mo(CO)_6$ and $Mn_2(CO)_{10}$ (RIC/ROC, United States) was carried out following the procedure described by Greco et al.,[11] according to the general reaction scheme:

$$n\mathrm{TiCl_4} + \mathrm{M(CO)}_x \rightarrow |\mathrm{M(CO)}_x \cdot n\mathrm{TiCl_4}| \rightarrow \mathrm{MnCl_4}n\mathrm{TiCl_3} + x\mathrm{Co}\nearrow \quad (1)$$

Well-defined stoichiometric adducts of $TiCl_3$ with MCl_x showing high activity for ethylene polymerization were prepared.

The $TiCl_3$ grade AA from Stauffer Chemical Co. was used without any modification or purification.

The supported catalysts containing Ti metal were prepared by previous treatment of the silica gels at 150°C under vacuum for 4 h. Then, the SiO_2 were reacted with a 7*M* solution of $TiCl_4$ in *n*-heptane under stirring (80 rpm) at 60°C during 3 h, using a ratio of 1 g SiO_2/2 mL $TiCl_4$. After the impregnation was finished, the excess of solution was vacuum eliminated. Then, it was washed with plenty of *n*-heptane and the solid catalysts dried at room temperature for 1 h. All the procedures were carried out in dry box or under N_2 blanket in order to assure anaerobic and anhydrous conditions. The total amount of supported Ti was determined as its peroxide by a colorimetric method using an ultraviolet Unicam SP 1800 Spectrometer.

Surface Area and Pore Size Determinations. The surface areas of the supported catalysts were determined by the well-established BET method.[12] First, the samples were evacuated at 10^{-4} torr for 24 h at room temperature to remove physisorbed molecules. Then, nitrogen gas was admitted, and the pressure drop was measured. The determinations were made for P/P_0 between 0.05 and 0.3; where P is the measured pressure and P_0 is the saturating vapor pressure of the nitrogen.

The results were plotted according to the equation

$$\frac{P/P_0}{V(1-P/P_0)} = \frac{1}{V_mC} + \frac{C-1}{V_mC} \times \frac{P}{P_0} \tag{2}$$

where V is the volume at pressure P, V_m is the volume of N_2 corresponding to the monolayer, and C is the BET constant.

The surface area S is determined by the following equation:

$$S = \frac{V_mAs}{W(22{,}400)} \text{ m}^2\cdot\text{g}^{-1} \tag{3}$$

where V_m has been previously calculated by eq. (2), A is the Avogadro's number, s is the area of one nitrogen molecule taken as 16.2×10^{-20} m^2, and W is the sample weight (g).

The pores size distribution was calculated by the adsorption–desorption isotherms using the Brunauer–Mikhail–Bodor method,[13] which is applied to pores of any shape. The determinations were made for values of P/P_0 until 1.0.

The total surface acidity (Lewis and Brøston acid centers) was determined by the Webb method,[14] using the chemisorption of NH_3 gas and given as mmol of NH_3/g of solid.

Polymerization Procedure. The polymerization procedures have been described elsewhere.[15] Careful precautions were taken to ensure anaerobic and anhydrous conditions. Polymerizations were conducted in batch in a 250-mL stirred glass autoclave (Büchi, Switzerland). Except where otherwise noted, the runs were carried out in *n*-heptane at constant ethylene pressure of 5 atm at 50°C and under 1200 rpm stirring speed in order to minimize mass transfer control of the polymerization rate, and normally using an |Al|/|Ti| ratio of 10. Both catalyst components, solid containing Ti and the Et_2AlCl used as cocatalyst, were introduced into the reactor separately. First, the cocatalyst was introduced and then the catalyst containing Ti.

Polymer Characterization. Viscosimetries were performed in Ubbelohde suspended level instruments. The intrinsic viscosity of the samples were determined at 135 ± 0.05°C in decalin containing 0.1 wt % of Santonox to avoid polymer degradation. The molecular weights were calculated by the equation[16]

$$|\eta| = 6.2 \times 10^{-4}\, \overline{M}_v^{0.70} \text{ (dL/g)} \tag{4}$$

Electron Microscopy. The catalysts and the polyethylene samples were examined in a scanning electron microscope (SEM) Philips SEM 500, using an accelerating voltage of 20 kV. The specimens were previously deposited on SEM stubs, joined by conductive–adhesive silver paint and coated with a film of gold about 20 Å by sputtering techniques in order to avoid electrostatic discharges during observations. General views of the samples for size and shape catalysts and polymer particles determinations were taken using an electron beam di-

ameter between 640 and 320 Å, while, for morphological detailed observations, smaller electron beam diameters of 80–160 Å were used, obtaining under the latest conditions higher resolutions at higher magnifications.

The preparations of the samples for observation under the transmission electron microscope (TEM) were made in the usual manner. Before viewing, the polyethylene samples were disrupted mechanically in ethanol by ultrasonic desintegrator. Subsequently, drops of the obtained suspension were dried on grids previously coated with a film of evaporated carbon. Then, the specimens were shadowed with Pt–C at an angle of 35° to improve the contrast.

Finally, the specimens were examined in a transmission electron microscope Philips TEM 201 at 100 kV acceleration voltage.

RESULTS AND DISCUSSION

Catalyst Composition and Kinetic Behavior

According to extensive studies,[7] when $TiCl_4$ is mixed with $AlEt_2Cl$, a series of reactions take place which involve reductions, alkylations, and dealkylations of the titanium, as shown in

$$TiCl_4 + AlEt_2Cl \rightarrow EtTiCl_3 + AlEtCl_2 \quad (5)$$

$$TiCl_4 + AlEtCl_2 \rightarrow EtTiCl_3 + AlCl_3 \quad (6)$$

$$EtTiCl_3 \rightarrow TiCl_3 + Et^{\cdot} \quad (7)$$

$$2Et^{\cdot} \rightarrow \text{ethane} + \text{ethylene} \quad (8)$$

The so-produced brown catalytic solid is very complex in its chemical composition, consisting of β-$TiCl_3$ mixed with $AlCl_3$ and probably with some chemisorbed $AlEtCl_2$.

This catalyst is very unstable and undergoes several reactions during the polymerization, which leads to its deactivation. This behavior is the main reason for the decay type curve observed for ethylene polymerization, as shown in Figure 1. The initial part of the curve could not be detected, owing to the formation of very high active centers immediately after the catalyst formation, which produces a very high polymerization activity. Therefore, only the decay period during which the activity decreases gradually has been represented.

In case of the reduction of $TiCl_4$ with the metal carbonyls $Mn_2(CO)_{10}$ and $Mo(CO)_6$, the produced catalytic solids show the chemical composition of $MnCl_2 \cdot 2TiCl_3$ and $MoCl_3 \cdot 3TiCl_3$, respectively, according to Greco et al.'s finding.[11] The $MoTi_3Cl_{12}$, having probably a mixture of β and γ modification of $TiCl_3$ is brown in color, while the $MnTi_2Cl_8$ presents the γ modification and is red-violet.

The polymerization kinetic curves obtained with these two catalytic systems are also of the decay type, but in these cases the build-up periods could be recorded. This might be due to the formation of more stable and probably less active centers than those produced in the $TiCl_4$–$AlEt_2Cl$ system. Thereupon, the deactivation of the active centers occurs slower. Finally, the activity obtained with the system containing Mo is lower than with Mn, as previously established by Greco et al.[11] In the case of $TiCl_3$–AA/$AlEt_2Cl$ also a decay type curve was

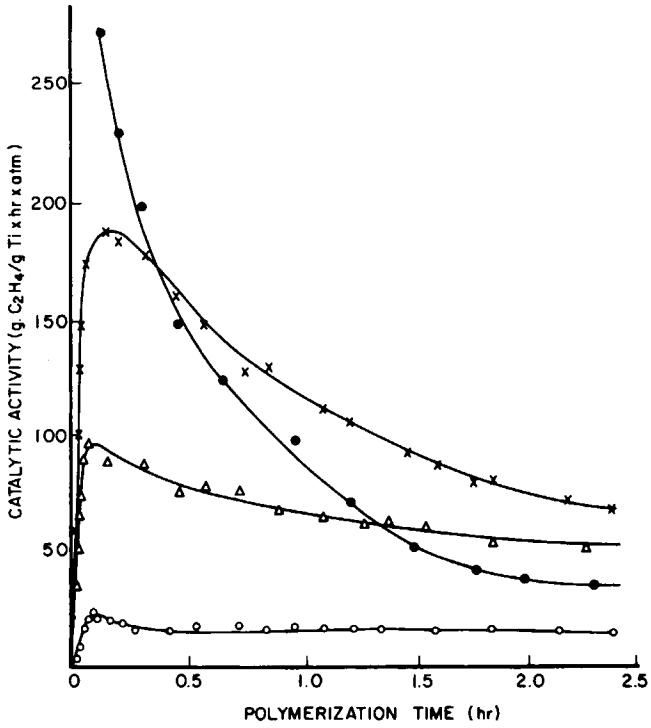

Fig. 1. Dependence of activities with the polymerization time observed for different catalysts: (○) $TiCl_4$ reduced with $AlEt_2Cl$; (△) $TiCl_3$–AA; (●) $TiCl_4$ reduced with $Mo(CO)_6$; (×) $TiCl_4$ reduced with $Mn_2(CO)_{10}$.

found, although with this catalytic system usually acceleration type curves have been reported.[17] The apparent disagreement with the results obtained in this work can be explained by the high |Al|/|Ti| ratio used for activation (i.e., 10 instead 4). This might produce a more intensive attack of $AlEt_2Cl$ to the active centers placed on the surface of the $TiCl_3$, poisoning and reducing the Ti(III) to a lower valence state.

The reason for using so high a |Al|/|Ti| ratio in the present work is owing to the necessity of comparing the results obtained with the previous unsupported conventional catalytic systems with the supported ones. With the later systems, the higher activities were achieved at |Al|/|Ti| ratios over 20[18]; nevertheless, as a compromise a ratio of 10 was chosen.

Another explanation given for the slow down of the catalytic activity is the encapsulation of the catalyst particles by the forming polymer, as the reaction proceeds. As a consequence of that, the polymerization becomes diffusion controlled. However, as will be referred to later on, this interpretation only does not give a consistent explanation to the results found for the supported catalysts. For these catalytic systems acceleration curves were found, proceeding the reaction at constant rate for several hours, although their activities are higher than those observed for the unsupported catalysts and therefore the polymer amount.

The preparation of supported Ziegler–Natta catalysts on SiO_2 carriers is based

on the reaction of $TiCl_4$ with isolated, vicinal, and geminal hydroxyl groups of the silica, according to the following equations[19-21]:

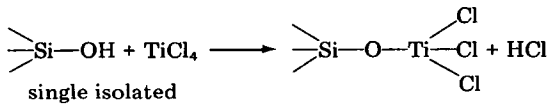

(9)

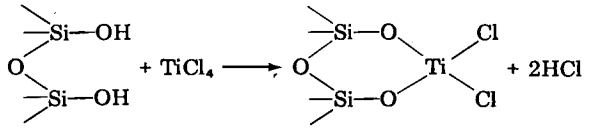

(10)

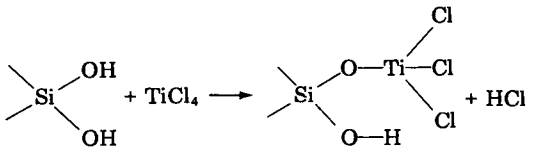

(11)

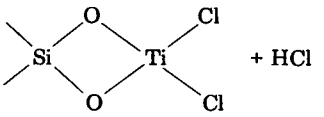

(12)

The amounts of Ti supported on the three different silicas are given in Table I. The higher amount of Ti (8.4%) deposited corresponds to the SiO_2 Davison 952, which is the more porous silica, and the lower Ti supported corresponds to the silica Dart 1000. It is also noteworthy that, during the reaction of $TiCl_4$ with SiO_2, approximately 0.4% of Ti(IV) is reduced to the oxidation state Ti(III). Furthermore, the original surface area of the SiO_2 is reduced significantly, while the surface area acidities increase. By subsequent reaction of the supported $TiCl_4$ on SiO_2 with the cocatalyst $AlEt_2Cl$, the following probable active species might be formed:

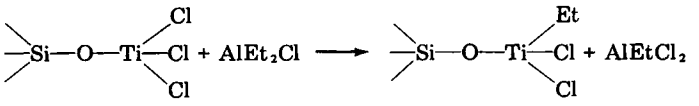

(13)

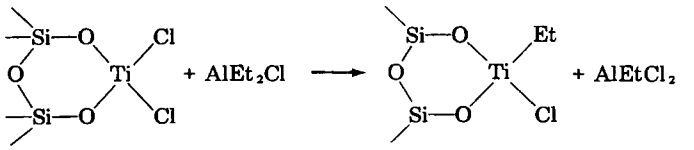

(14)

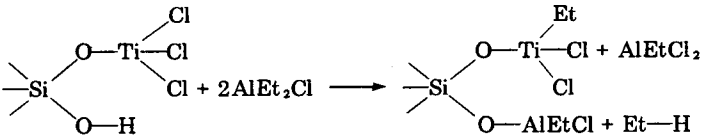

(15)

(16)

TABLE I
Characteristics of the SiO_2 Used as Carriers and Their Modification after Deposition of $TiCl_4$

	Silicas before impregnation			Catalysts with $TiCl_4$ supported		
Samples	Surface area (m^2/g)	Acidity (mmol NH_3/g)	Pore volume (mL/g)	% Ti	Surface area (m^2/g)	Acidity (mmol NH_3/g)
Davison 951	611	0.35	0.90	6.7 ± 0.5	350 ± 27	5.2 ± 0.4
Davison 952	220	0.40	1.60	8.4 ± 0.7	190 ± 14	3.3 ± 0.3
Dart 1000	260	0.56	1.50	4.6 ± 0.4	200 ± 15	4.2 ± 0.3

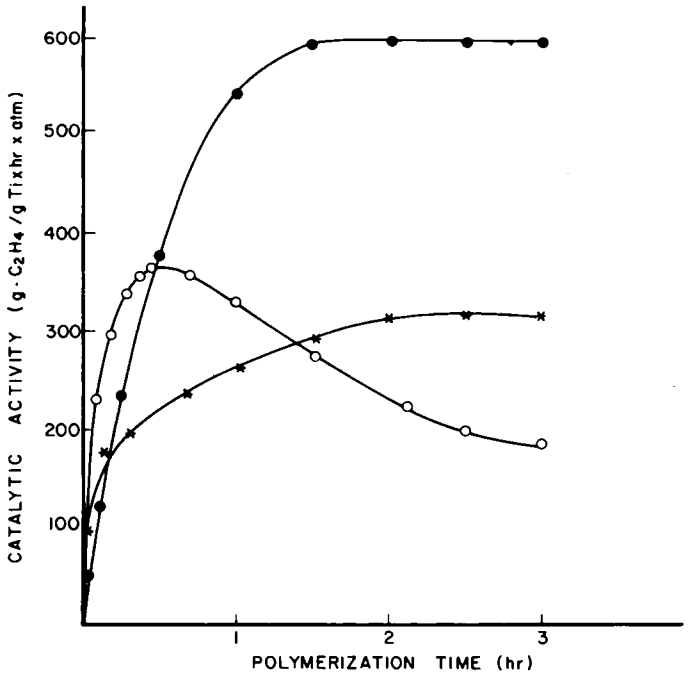

Fig. 2. Dependence of the activities with the polymerization time observed for the three supported $TiCl_4$ catalysts on three different silicas: (*) Dart 1000; (●) Davison 952; (○) Davison 951.

Single alkylation reactions have been formulated, but double and even triple alkylations of the titanium might be also considered. Furthermore, it has been shown[18] that a certain amount of the surface bounded Ti(IV), situated in close proximity to one another, can be reduced to Ti(III) by the aluminum alkyl reaction. These species might also participate in the polymerization of ethylene.

The kinetic curves for the three supported catalytic systems are given in Figure 2. It can be observed that the activities for the supported catalysts are higher than the activities found for the unsupported ones. This might be due to an increase in the number of "working titanium" by spreading them out on the supports. On the other hand, the activity and also the kinetic behavior depend on the type of silica used. For the Davison 951 and Dart 1000, acceleration-type curves were obtained, while for the Davison 952 a decay curve was found.

The following conclusions may be drawn from the above results: First, the decay period in the decay type polymerizations might be due mainly to deactivation processes of the catalytic active centers, rather than to diffusion controlled reactions. This is especially true when a low amount of polymer is formed. Second, the acceleration curves observed for catalysts supported on 951 and 1000 silicas may be due to the formation of more stable and evenly distributed active centers on the catalyst surface. Third, the decay type curve found for the catalyst using 952 silica might be explained by admitting aggregations of active center by a poor dispersion of the titanium. In this case, deactivation between active centers might occur by the following equations:

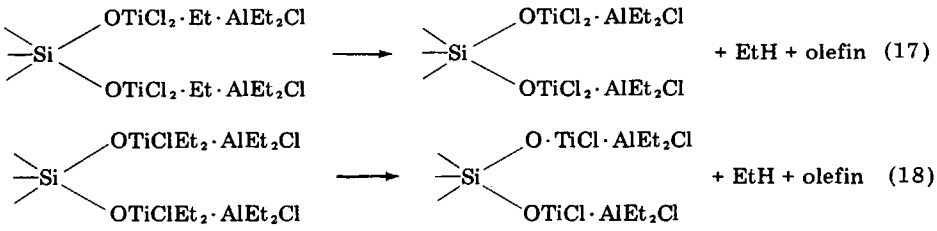

giving Ti in a less active oxidation state. On the other hand, the 952 SiO_2 particles have poor mechanical strength undergoing disruption and pulverization into very fine particles.

Finally, the polyethylene molecular weights obtained with different catalytic systems are given in Table II. It can be seen that in absence of H_2 the molecular weights are in the range of the ultra-high-molecular weight polyethylenes (UHMWPE).

Morphology of the Polymer Granules

SEM micrographs of polyethylene powder obtained by slurry polymerization of ethylene in *n*-heptane using $TiCl_4$ and reduced with $AlEt_2Cl$ showed that this conventional catalytic system has a very poor control on the size and shape of the polymer particle. The granules are irregular, rough, and spongy, with very low bulk density of about 0.100 kg·L^{-1} [Fig. 3(a)]. However, when the |Al|/|Ti| ratio increases the produced polymer particles are more dense, smooth and nearly spherical [Fig. 3(b)]. In addition to this, the size also increases, as can be seen in Table III. At higher magnifications, different interesting features could be observed. The particles exhibit a globular morphology, i.e., they are formed by

TABLE II
Polyethylene Molecular Weights Obtained with Different Catalytic Systems

Catalytic system	Molecular weight ($M_v \times 10^{-6}$)
$TiCl_4/AlEt_2Cl$	1.26
$TiCl_4/Mo(CO)_6/AlEt_2Cl$	2.95
$TiCl_4/Mn_2(CO)_{10}/AlEt_2Cl$	1.95
$TiCl_4/951SiO_2/AlEt_2Cl$	2.65

TABLE III

Catalytic system	|Al|/|Ti|	Average size (μ)
$TiCl_4/AlEt_2Cl$	5	100–200
$TiCl_4AlEt_2Cl$	10	200–400
$TiCl_4/AlEt_2Cl$	30	300–500
$TiCl_4/M(CO)_x/AlEt_2Cl$[a]	10	50–300
$TiCl_3(AA)/AlEt_2Cl$	5	100–300
$TiCl_4/SiO_2/AlEt_2Cl$	30	200–500[b]

[a] Where $M = M_n$ and M_0.

[b] It depends on the original size of the catalytic support SiO_2.

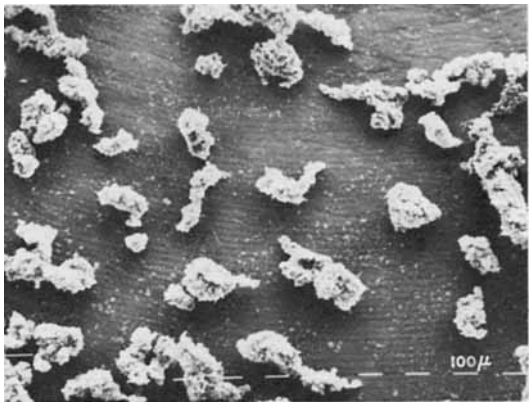

(a)

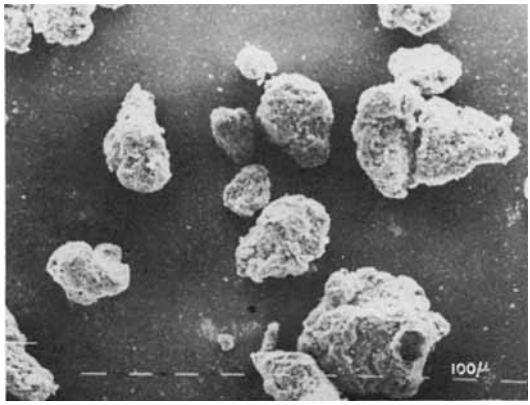

(b)

Fig. 3. SEM micrographs of polyethylene particles obtained with the $TiCl_4$ reduced with $AlEt_2Cl$ at different |Al|/|Ti| ratios: (a) 5; (b) 30.

aggregations of globules, interconnected each other by fibers, which are originated by stretching the polymer between them due to expansion of the particles during growth (Fig. 4). Furthermore, it can be seen that the globules display a clear lamellar characteristic.

Similar observations were obtained with the catalytic systems based on $TiCl_4$ reduced with metal carbonyls [$Mn_2(CO)_{10}$ and $Mo(CO)_6$] and activated with $AlEt_2Cl$ [Fig. 5(a)]. However, in the case of the catalyst containing Mo, a wormlike morphology, as shown in Figure 5(b), was observed. On the other hand, the bulk densities of these polymers are lightly higher and the particle size distribution broader (see Table III).

The polymer granules produced with the $TiCl_3$–AA/$AlEt_2Cl$ catalytic system are similar in size to those obtained with the previous catalytic system (Table III), at the same |Al|/|Ti| ratio. However, they are more regular in shape and more dense, having a bulk density of about 0.300–0.350 kg·L^{-1}.

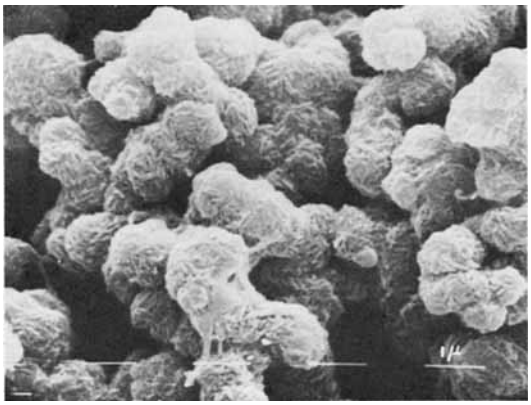

Fig. 4. SEM micrographs of the globular morphology obtained by the slurry polymerization of ethylene using the $TiCl_4$–$AlEt_2Cl$ catalyst.

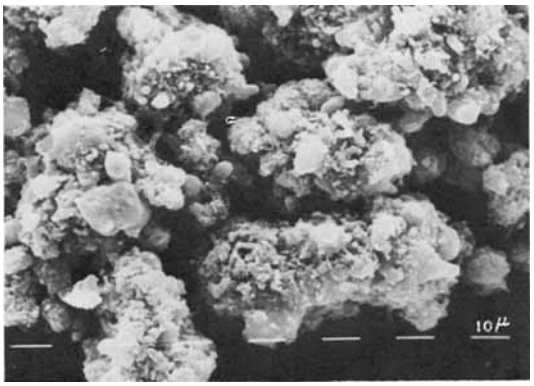

(a)

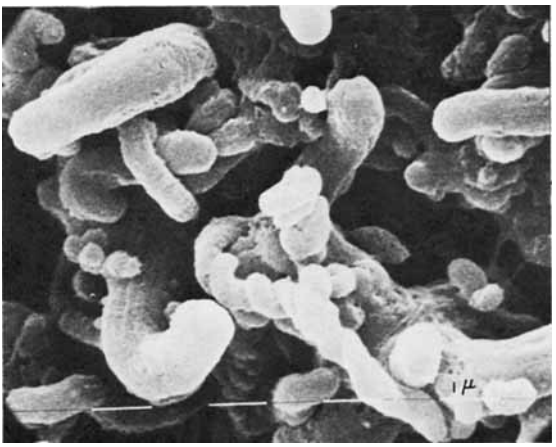

(b)

Fig. 5. (a) SEM micrographs of polymer particles and (b) wormlike morphology observed by the polymerization of ethylene using the $TiCl_4$–$Mo(CO)_6$ catalyst system.

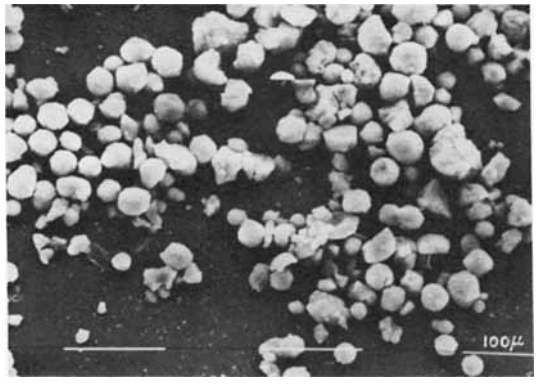

(a)

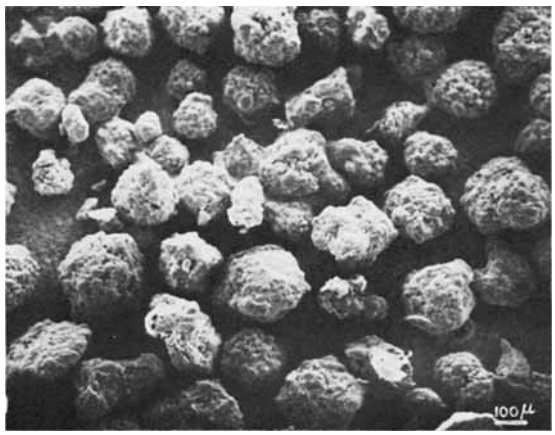

(b)

Fig. 6. (a) SEM micrographs of the silica Davison 951 before polymerization and (b) of the resulting polymer beads.

Finally, the supported catalysts on SiO_2 showed the best catalytic control on the size and shape of the polymer particles (Fig. 6–8). The bulk densities are in the range of about 0.400–0.450 $kg \cdot L^{-1}$. Furthermore, when the SiO_2 aggregates have low mechanical strength, due to the fact that the primary particles are bonded together at a low degree of coalescence, they undergo dispersion into finer aggregate, giving rise to smaller polymer particles, broadening the particles size distribution, and increasing the amount of fines in the polymer. This is the case of the 952 SiO_2 and to a lesser degree of the Dart 1000. On the other hand, the higher polymer–catalyst average particle-size replication ratio corresponds to the catalyst obtained with the 952 SiO_2 having a value of 25, while the replication factors of the other catalysts were 10 and 5 for the Davison 951 and Dart 1000, respectively (Fig. 9). For comparison Luciani et al.[22] have reported polymer–catalyst replication ratios as high as 39–27, while Galli et al.[9] have published values in the order of 20 using $MgCl_2$-supported $TiCl_4$ catalyst. These values contrast with 7–10 of the traditional catalysts.

Furthermore, it has been found that Davison 951 is the silica giving the best control of the shape and size distribution of the polymer [see Fig. 6(b)]. This

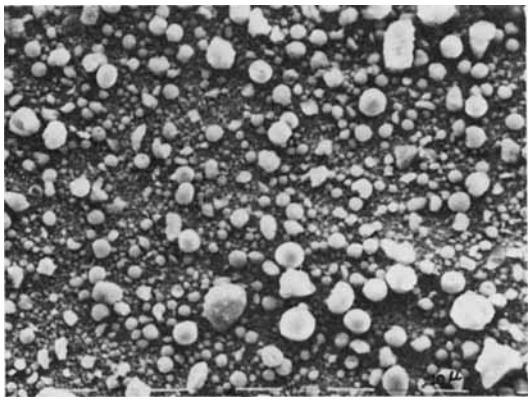

(a)

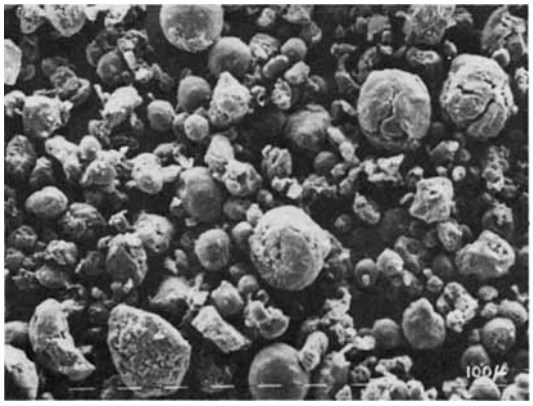

(b)

Fig. 7. (a) SEM micrographs of the silica Davison 952 before polymerization and (b) of the resulting polymer beads.

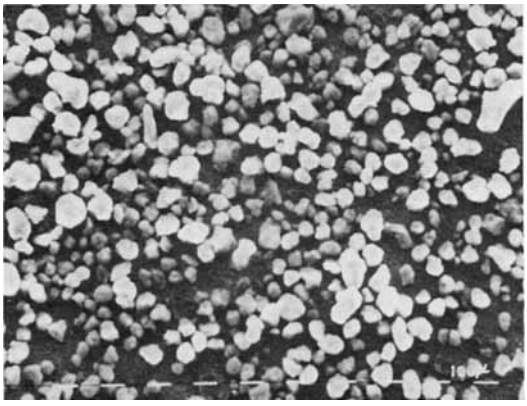

(a)

Fig. 8. (a) SEM micrographs of the silica Dart 1000 before polymerization and (b) of the resulting polymer beads.

(b)

Fig. 8 (*Continued from the previous page.*)

is mainly due to the more uniformity in the size of the silica granules and also to its best mechanical strength, avoiding the formation of fine particles by disruption of the catalyst during polymer growth.

On the other hand, it was observed that a certain amount of polymer produced with the silica Davison 952 consists of hollow spherical beads, as can be seen in Figure 7(b). This is so, although the silica granules are apparently solids. Akar

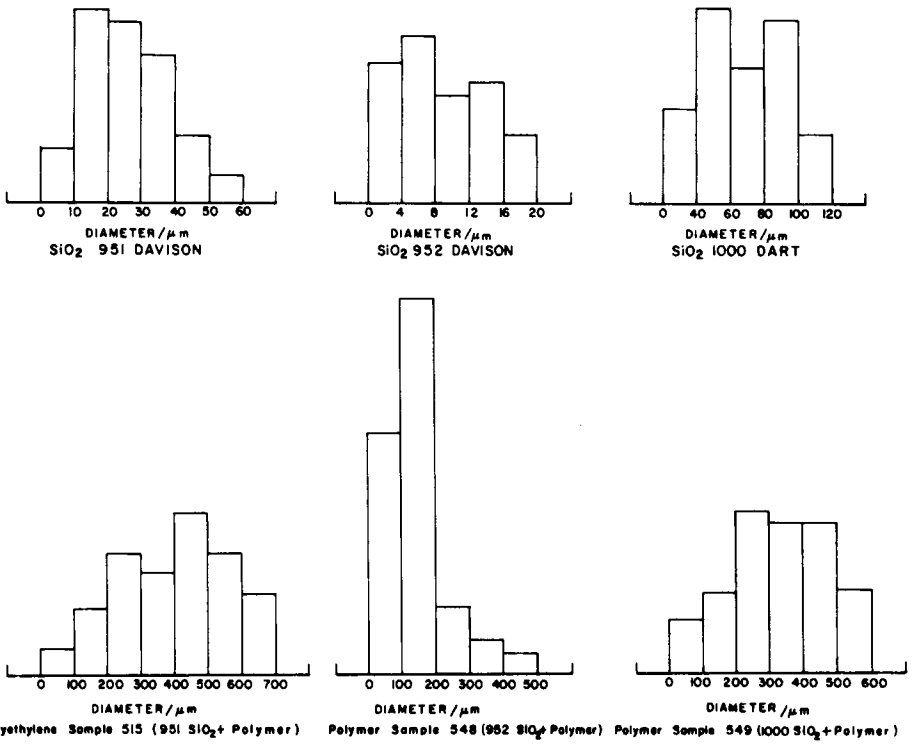

Fig. 9. Approximate size distribution for the silica used as supports and for the resulting polymer beads.

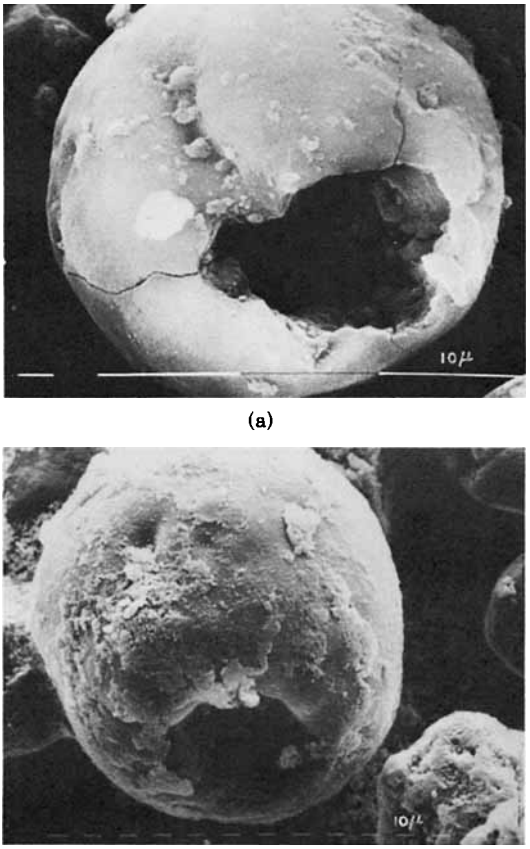

(a)

(b)

Fig. 10. SEM micrographs of the (a) hollow catalyst bead and (b) of the resulting replicated polymer bead.

et al.[23] have found similar results in the ethylene polymerization using organometallic compounds, such as zirconium tetrabenzyl, supported on alumina. These authors suppose that the only reason for this result is a special mechanism that takes place by the nonuniform polymerization of the ethylene on the supported catalyst. The polymerization occurs faster on the outside of the catalyst beads than on the inner surface, as a consequence of the diffusion limitation of the monomer in the very early stages of the reaction. The outer layers of the beads undergo expansion more rapidly producing the hollow polymer granules. Our results are rather different.

In this case, the hollow polymer beads are produced due to the fact that there were hollow particles already present in the catalyst, imposing their shape to the polymer by the replication phenomenon, as shown in Figure 10. It can be seen that, although the polymer bead is approximately 10 times bigger than the catalyst, it retains the hollow shape.

Finally, further insight into the fine morphology of the polymer particles was possible to obtain using TEM techniques. It was found that the globular morphology is produced by catalysts which are formed by subparticles linked by

strong forces and its activity is not very high. On the other side, the wormlike morphology was observed when the catalyst subparticles were very active in the polymerization and the force linking them together was weaker.

References

1. L. A. M. Rodríguez and J. A. Gabant, *J. Polym. Sci. Part C-4*, 125 (1964).
2. P. Mackie, M. N. Berger, B. M. Grieveson, and D. Lawson, *J. Polym. Sci. Part B-1*, **5**, 493–494 (1967).
3. Farbwerke Hoechst, Br. Pat. 960,232 (1964).
4. P. Blais and R. St. John Manley, *J. Polym. Sci. Part A-1*, **6**, 291 (1968).
5. J. Y. Guttman and J. E. Guillet, *Macromolecules*, **1**, 461 (1968).
6. H. D. Chanzy, B. Fisa, and R. H. Marchessault, *Crit. Rev. Macromol. Sci.*, **1**(3), 315 (1973).
7. J. Boor, Jr., *Ziegler-Natta Catalysts and Polymerization*, Academic, New York, 1979.
8. A. Muñoz-Escalona, C. Villamizar, and P. Frías, in *Structure–Properties Relationship of Polymeric Solids*, A. Hiltner, Ed., Plenum, New York, 1983.
9. P. Galli, L. Luciani, and G. Cecchin, *Angew. Makromol. Chem.*, **94**, 63 (1981).
10. A. Muñoz-Escalona and A. Parada, *J. Cryst. Growth*, **48**, 250 (1980).
11. A. Greco, G. Perego, M. Cesari, and S. Cesca, *J. Appl. Polym. Sci.*, **23**, 1319 (1979).
12. S. Brunauer, P. H. Emmet, and E. Teller, *J. Am. Chem. Soc.*, **60**, 309 (1938).
13. S. Brunauer, R. S. Mikhail, and E. E. Bodor, *J. Colloid Interface Sci.*, **24**, 451 (1967).
14. A. N. Webb, *Ind. Eng. Chem.*, **49**, 261 (1957).
15. A. Muñoz-Escalona and J. Villalba, *Polymer* **18**, 179 (1977).
16. R. J. Chiang, *J. Phys. Chem.*, **69**, 1945 (1965).
17. T. Keii, *Kinetics of Ziegler-Natta Polymerization*, Chapman and Hall, London, 1972.
18. A. Muñoz-Escalona, to appear.
19. J. Murray, J. J. Sharp, and J. A. Hockey, *J. Catal.*, **18**, 52 (1970).
20. J. C. W. Chien, *J. Catal.*, **23**, 71 (1971).
21. A. Muñoz-Escalona, in *Transition Metal Catalyzed Polymerizations. Alkene and Dienes*, R. P. Quirk, Ed., MMI Press, Mich., 1983.
22. L. Luciani, G. Foschini, C. Cipriani, and Ch. A. Trischman, Soc. Plast. Eng. Tech. Conf. (ANTEC), San Francisco, 1982, p. 220.
23. A. Akar, N. C. Billingham, and P. D. Calvert, in *Transition Metal Catalyzed Polymerizations. Alkene and Dienes*, R. P. Quirk, Ed., MMI Press, Mich., 1983.

Received September 8, 1983
Accepted September 16, 1983